Critical point relascope sampling for unbiased volume estimation of downed coarse woody debris

JEFFREY H. GOVE[1]*, MICHAEL S. WILLIAMS[2], GÖRAN STÅHL[3] AND MARK J. DUCEY[4]

[1]Northeastern Research Station, USDA Forest Service, 271 Mast Road, PO Box 640, Durham, NH 03824, USA
[2]Rocky Mountain Research Station, USDA Forest Service, 2150 A Centre Avenue, Suite 361, Fort Collins, CO 80526, USA
[3]Department of Forest Resource Management and Geomatics, Swedish University of Agricultural Sciences, SE-901 83 Umeå, Sweden
[4]Department of Natural Resources, 221 James Hall, University of New Hampshire, Durham, NH 03824, USA
*Corresponding author. E-mail: jgove@fs.fed.us

Summary

Critical point relascope sampling is developed and shown to be design-unbiased for the estimation of log volume when used with point relascope sampling for downed coarse woody debris. The method is closely related to critical height sampling for standing trees when trees are first sampled with a wedge prism. Three alternative protocols for determining the critical sampling points on a log are presented and simulations are employed to suggest the most efficient protocol to use in practice.

Introduction

Point relascope sampling (PRS) was introduced by Gove *et al.* (1999) as a method to sample downed coarse woody debris (CWD) in forest inventories using a wide-angle gauge, with angle $0° < \nu \leq 90°$. The appeal of such a method is that it is unbiased, and is closely linked to horizontal point sampling (HPS) with a prism or small-angle gauge for standing-tree inventories (Grosenbaugh, 1958). A transect-based alternative to PRS, known as transect relascope sampling, was introduced first by Ståhl (1998), and is analogous to horizontal line sampling for standing trees using a prism along a transect. These methods have been developed to the point where most auxillary problems that might be encountered in the field, such as slope correction (Ståhl *et al.*, 2002), boundary overlap (Gove *et al.*, 1999; Ducey *et al.*, 2004) and branchiness (Gove *et al.*, 2002), have been addressed. However, volume estimation under these methods normally entails using some type of model for log taper and applying a formula such as Smalian's (Husch *et al.*, 2003, p. 122) to approximate the volume of individual logs. The use of Smalian's formula (or similar cubic content models), which assumes that the log is a frustum of a parabola, introduces a bias of unknown magnitude and sign into the estimation of volume.

© Institute of Chartered Foresters, 2005. All rights reserved.
For Permissions, please email: journals.permissions@oupjournals.org

Forestry, Vol. 78, No. 4, 2005. doi:10.1093/forestry/cpi040
Advance Access publication date 1 July 2005

Various methods are available for unbiased estimation of log volume. Probably the most well-known options are the variants of importance sampling. Importance sampling is a subsampling technique that chooses to sample points along the log, based on a simple taper model proxy function (Furnival *et al.*, 1986). Subsampling points are chosen in accord with the proxy taper function such that measurements are concentrated in the parts of the log with larger cross-sectional area. When CWD is branched, importance sampling in combination with randomized branch sampling might be employed (Valentine *et al.*, 1984). For standing trees, critical height sampling (CHS) (Kitamura, 1962) provides unbiased estimates of volume under HPS inventories. Recently, a new method, perpendicular distance sampling (PDS), has been introduced for the unbiased estimation of downed CWD volume by Williams and Gove (2003). PDS is simple and quick, and can be used in concert with other methods such as fixed-area plot sampling, for example, to arrive at estimates for other quantities such as number of pieces, since PDS does not provide estimates of these quantities directly. In addition, Williams *et al.* (2005a, b) provide an extension to PDS for unbiased estimation of log surface area, methods for handling branched or curved logs and procedures for slope correction. Finally, Ståhl *et al.* (2005) have developed critical length sampling as another method for estimating volume of downed logs. Their method is also design-unbiased and utilizes a wedge prism to determine the critical lengths of logs.

In PRS, downed pieces of CWD (hereafter simply 'logs') are selected with the angle gauge with probability proportional to the log length squared. As mentioned above, PRS is analogous to HPS in this and many other ways, since HPS selects trees with probability proportional to diameter squared. This distinction makes sense because in the former the angle gauge is used to view log length for inclusion, while in the latter it is used to view tree diameter. Similarly, if one desires to estimate some total quantity Y for the tract such as the number of individuals, the corresponding estimators are

$$\hat{Y} = A\mathcal{L}\sum_{i=1}^{n}\frac{y_i}{L_i^2} \quad \text{and} \quad \hat{Y} = A\mathcal{F}\sum_{i=1}^{n}\frac{y_i}{\kappa d_i^2}$$

for PRS and HPS, respectively, where κ is a conversion factor, and the other quantities will be defined later – the important point here is the similarity in the form of the estimators. Since CHS produces unbiased estimates of tree volume under HPS, it is natural to wonder, because of the relationship between the two methods, whether some analogue is also possible under PRS. The purpose of this paper is to introduce a new design-unbiased method for volume estimation of downed logs in a PRS inventory, critical point relascope sampling (CPRS), that does indeed provide such an analogue. The remainder of this paper begins with a brief review of CHS to motivate the development of CPRS and provides a proof of design unbiasedness with three protocols, then finally provides some guidance on the best protocol to be used based on simulation experiments.

Critical height sampling

CHS was introduced by Kitamura (1962) as a method for unbiased estimation of standing-tree volume. Proof of unbiasedness for CHS as well as other enhancements and applications appear in Iles (1979a), McTague and Bailey (1985), Lynch (1986), Van Deusen and Merrschaert (1986) and Van Deusen (1987). In review, CHS works in concert with HPS by conditioning on the selection of a tree with the angle gauge or prism on a sample point. Given that the sample tree has been selected, the critical height can then be found, in theory, by sighting at that point on the stem where the gauge angle is exactly coincident to the tree diameter – i.e. in the borderline condition. This is often done in practice with a relascope.

Figure 1 is useful to illustrate the general idea behind CHS. This figure shows a hypothetical (branchless) tree stem, along with an expanded tree stem surface that has been generated as a factor times the diameter at any given point on the stem, where the expansion factor is related to the gauge angle used. The sample point is at the vertical line. The point where this vertical line intersects the expanded tree stem surface determines the critical point on the stem where the diameter is borderline, determining both the critical height and associated critical diameter. If the sample point were rotated around the tree at this point while maintaining tangency of the projected gauge angle, it would produce a circular region (assuming a circular tree cross-section at this

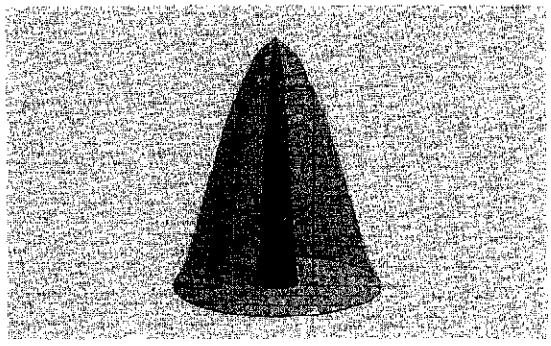

Figure 1. Illustration of CHS with the expanded tree stem (translucent), sample point (vertical line) and critical point (upper circle).

point) that would always select this critical height as shown by the upper circle in the figure. Denote the diameter of the tree at this critical point as d', and likewise, the diameter at the base of the tree as D. The circular borderline area at the tree base, proportional to D, is also shown.

The probability of selecting a critical point on the tree stem has been shown by several authors (McTague and Bailey, 1985; Lynch, 1986; Van Deusen and Merrschaert, 1986). Because it is useful to recall this result before developing CPRS in the next section, we briefly review it here. The cumulative distribution function that yields the probability of being closer to the centre of the selection circle defined by D, than a point on the expanded tree circle defined by the critical point d', is given by the ratio of the circular areas described above, viz.

$$P(d < d') = \frac{d'^2}{D^2}.$$

For the critical height estimator to be unbiased, tree selection, and thus the selection circle, must be at the lowest point on the tree containing the volume of interest, normally stump height, rather than breast height (Lynch, 1986; Van Deusen and Merrschaert, 1986; Van Deusen, 1987). The probability density function (PDF) of d is found by differentiation to be

$$p(d) = \frac{2d}{D^2}, \quad 0 < d < D.$$

Both Lynch (1986) and Van Deusen and Merrschaert (1986) have used this PDF and the shell integral to prove the unbiasedness for CHS for any tree taper function. Interested readers are referred to these papers for the details and the references therein. The final critical height estimator for volume on an individual sample point is

$$v_{\mathrm{ch}} = A\mathcal{F}\sum_{i=1}^{n} h_i,$$

where h_i is the critical height on the ith tree, n is the total number of 'in' trees selected on the point, A is the forest land area and $\mathcal{F}$ is the basal area factor of the angle gauge used (Kitamura, 1962; Iles, 1979a; Lynch, 1986).

CPRS theory and design

The development of CPRS is very similar to that of CHS. Conceptually, begin by conditioning on a log having first been selected with a wide-angle gauge under PRS as described in Gove *et al.* (1999). Because the log has already been chosen with the angle gauge, the log is longer than the projected angle of the gauge. Next, align one pin of the angle gauge (i.e. one side of the projected gauge angle) with either the small or large end of the log. The other pin on the angle gauge must therefore intersect the log at some point along its length. The point where this other pin of the angle gauge intersects the log determines a critical point on the log; this is shown with projected angles in Figure 2. This procedure can be thought of as being similar to scanning up a standing tree to the critical height on a tree that has already been selected on an HPS point. Thus, the critical point on the log determines a random sampling location on the log with associated critical length and diameter, just as CHS provides a critical height and associated diameter. In the following, it will be shown that the PDF for the critical point and a design-unbiased estimator for log volume estimation can be developed.

To illustrate the general idea, Figure 3 shows two inclusion zones for a log under PRS. The outside zone corresponds to the inclusion zone for the entire log as we would normally envision it under PRS (Gove *et al.*, 1999). The periphery of the smaller, internal zone delineates a locus of PRS

sample points where the same critical point on the log would be chosen by an angle gauge of $\nu = 50°$, when aligning one side of the gauge with the large end of the log. For simplicity, the following development of CPRS theory assumes that one side of the angle gauge is always aligned with the large end of the log as shown in Figures 2 and 3; however, this assumption will be relaxed subsequently.

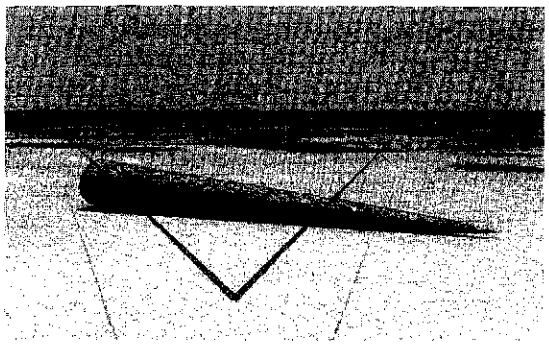

Figure 2. Illustration of CPRS with a wide-angle gauge. The critical point is where the gauge angle intersects the log (not the gauge's projected shadow, which is simply an artefact of the light sources used in ray tracing).

The development of the PDF for critical PRS follows directly from that of CHS. The probability of a random sampling point determining a length l that is shorter than some critical length l' for a sample log of total length L under PRS is given as

$$P(l < l') = \frac{\varphi l'^2}{\varphi L^2} = \frac{l'^2}{L^2},$$

where the dimensionless constant φ determines the log's inclusion area as the union of two overlapping circles (Gove *et al.*, 1999). By differentiation, the PDF is

$$p(l) = \frac{2l}{L^2}, \quad 0 < l \leq L. \tag{1}$$

The expected critical length under this PDF is $2L/3$ and the variance is $L^2/18$.

Let the total volume on the tract be given by summing the volumes on the individual downed logs, viz.

$$V = \sum_{i=1}^{N} v_i,$$

where v_i is the volume of the ith log, with N logs on the forest tract. Then an unbiased estimator for volume on the tract for a given point sample

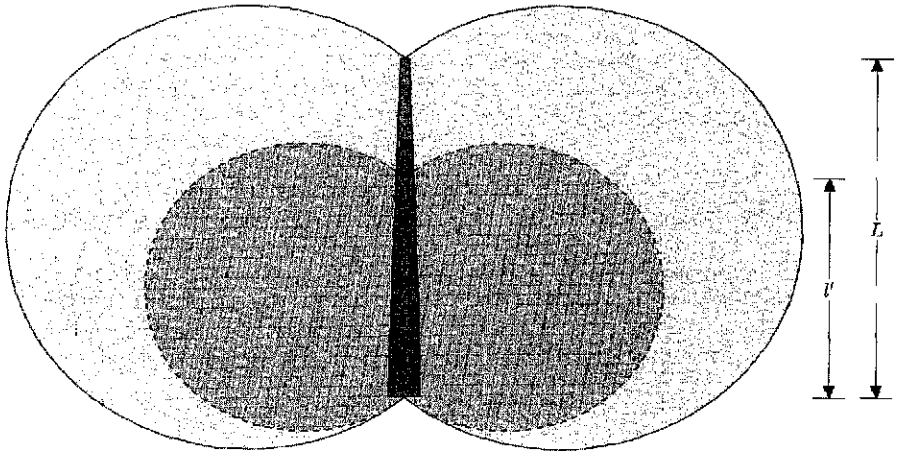

Figure 3. Illustration of the geometry of CPRS with an gauge angle of $\nu = 50°$ when sampling the log from the large end. A random PRS sample point falling anywhere on the inner (dashed line) inclusion zone boundary will always choose the same critical point on the log with associated length l'.

under PRS may be written in terms of the critical diameters and lengths of the sampled logs as

$$v' = cA\mathcal{L}\sum_{i=1}^{n}\frac{d_i'^2}{l_i'}, \quad l_i' > 0, \tag{2}$$

where n is the number of logs that are 'in' with the angle gauge on a PRS point, $\mathcal{L}$ is the PRS squared-length angle gauge factor (Gove *et al.*, 1999), A is the forest area in hectares, d_i' is the log diameter with the same units as length (i.e. metres) at the critical point and the constant c is a correction for unbiasedness as developed below.

In an inventory of downed CWD where PRS is used on p sample points, one typically desires some estimate of the variance for volume. In this case, let $\hat{v}_k'$ be the volume estimate by CPRS from n_k logs tallied on the kth sample point, then the volume of downed CWD would be unbiasedly estimated by

$$\hat{V} = \frac{1}{p}\sum_{i=1}^{p}\hat{v}_k'.$$

The associated variance estimator is given as

$$\mathrm{var}(\hat{V}) = \frac{1}{p(p-1)}\sum_{k=1}^{p}(\hat{v}_k' - \hat{V})^2.$$

Proof of estimator unbiasedness

The proof of unbiasedness for the estimator (2) of total log volume follows closely from the methods of Lynch (1986) and Van Deusen and Merrschaert (1986), who generalized the proof for CHS of standing trees given by McTague and Bailey (1985). Let t_i be an indicator random variable that takes the value 1 if the log is selected under PRS and 0 otherwise. Then the CPRS estimator of volume for a single PRS point can be written as

$$v' = cA\mathcal{L}\sum_{i=1}^{N}\frac{d_i'^2}{l_i'}t_i, \quad l_i' > 0.$$

To prove unbiasedness, the expectation is taken, viz.

$$\begin{aligned}\mathrm{E}[v'] &= cA\mathcal{L}\sum_{i=1}^{N}\mathrm{E}\left[\frac{d_i'^2}{l_i'}\,|\,t_i = 0\right]P(t_i = 0) \\ &\quad + \mathrm{E}\left[\frac{d_i'^2}{l_i'}\,|\,t_i = 1\right]P(t_i = 1) \\ &= cA\mathcal{L}\sum_{i=1}^{N}\mathrm{E}\left[\frac{d_i'^2}{l_i'}\,|\,t_i = 1\right]P(t_i = 1),\end{aligned}$$

where $P(t_i = 1) = \frac{L_i^2}{A\mathcal{L}}$ is the probability of sampling a log of length L_i under PRS (Gove *et al.*, 1999).

An invertible taper function is assumed for the log such that $l(d')$ and $d(l')$ both denote the same critical point on the log. Because of the taper function constraint, one of the variables (l', d') is viewed as random and the other as fixed, as the situation dictates, as in regression. In addition, in the following, the substitution $d_i^2 = 4r_i^2$ is made, acknowledging that the same relationships hold between radius and length as between diameter and length in the taper functions. Thus,

$$\begin{aligned}\mathrm{E}\left[\frac{d_i'^2}{l_i'}\,|\,t_i = 1\right] &= \frac{4}{l_i'}\int_0^{L} r_i^2(l)\frac{2l_i'}{L_i^2}\,\mathrm{d}l \\ &= \frac{8\pi}{\pi L_i^2}\int_0^{L} r_i^2(l)\,\mathrm{d}l \\ &= \frac{v_i}{cL_i^2},\end{aligned}$$

where $c = \pi/8$ is a constant factor that ensures estimator unbiasedness. The penultimate step above follows from the formula for the volume for a solid of revolution by the disk method from the calculus (Mizrahi and Sullivan, 1982, p. 309). Therefore, the estimator is unbiased, since

$$\begin{aligned}\mathrm{E}[v'] &= cA\mathcal{L}\sum_{i=1}^{N}\frac{v_i}{cL_i^2}\frac{L_i^2}{A\mathcal{L}} \\ &= \sum_{i=1}^{N} v_i.\end{aligned}$$

Note in the above proof that the quantity v_i/L_i^2 is a volume-to-length squared ratio, much like the volume-to-basal area ratio that results from the critical height proofs under HPS.

Designing the estimator protocol

In the proof of the last section, it was assumed that one pin of the angle gauge was always aligned with the large end of the log in question. It should be clear that unbiasedness can similarly be proven when the assumption is made that one pin of the angle gauge is aligned with the log's small end instead. What may not be immediately obvious, however, is that it does make a difference whether the gauge is aligned consistently with the log's large or small end when considering the variance of the estimator. Because a similar form of the

estimator (2) is used in either case, this stage in the development concerns the sampling protocol, and possible associated reduction in variance that can be obtained by judicious choice of gauge alignment when subsampling for critical length using CPRS.

Williams (2001) presented a method based on simulation that allows the visualization of the surface that results from sampling at all possible locations on a grid. Direct computation of means and variances are possible, facilitating comparison of different estimators and protocols. In brief, assume that one or more logs are distributed onto a plane $\mathcal{A}$, with area A, that has been tessellated into a grid. At each grid cell, and for each log, a test is made as to whether the log is to be selected under PRS. If a given log is 'in', the critical point for that log is determined with the gauge angle used, and the value of the grid cell is assigned based on equation (2) with $n = 1$. When more than one log is selected at a given grid cell ($n > 1$), the value obtained is the sum of the values for the selected logs as in equation (2). In this way, a surface is built up for all grid cells – the resulting surface is known as the *sampling surface* (Williams, 2001). Sampling in this way is exhaustive for a given grid size, because it is like visiting each grid cell, establishing a PRS point at its centre and calculating the estimated volume under the CPRS estimator for that point location. Evidently, geometrically similar methods were used with regard to CHS by both Kitamura (1962) and Iles (1979b).

Assume that $\mathcal{A}$ has been divided into m sampling locations, or grid cells, and let the estimated value of the surface under CPRS at cell (x, y) be given as $\hat{v}(x,y)$. Then the mean and variance of the surface are estimated as

$$\bar{V} = \frac{1}{m}\sum_{i=1}^{m}\hat{v}(x, y)$$

and

$$\mathrm{var}(\hat{v}(x, y)) = \frac{1}{m-1}\sum_{i=1}^{m}(\hat{v}(x, y) - \bar{V})^2, \qquad (3)$$

respectively. The finer the mesh of the grid, the closer the simulated estimates will be to the true values of the population parameters they estimate. To reiterate, these are essentially the traditional Monte Carlo estimators with all possible samples under repeated sampling without replacement, when sample points are restricted to falling at the centre of each grid cell. In addition, as the grid cell size goes to zero, the sampling surface becomes analogous to the infinite population Monte Carlo methods described in Valentine *et al.* (2001).

To facilitate the sampling surface simulations, artificial logs or populations of logs were generated. The taper and associated total log volume equations used in the sampling surface simulations are from Van Deusen (1990), and allow for logs with various taper models and non-zero small-end diameters, viz.

$$\begin{aligned} l(d) &= L - L\left(\frac{d - d_u}{d_l - d_u}\right)^{r/2}, \\ d(l) &= d_u + (d_l - d_u)\left(\frac{L - l}{L}\right)^{2/r}, \end{aligned} \qquad (4)$$

with

$$V = \pi k L\left[(d_l - d_u)^2\left(\frac{r}{r+4}\right) + d_u\left(d_u + 2(d_l - d_u)\left(\frac{r}{r+2}\right)\right)\right], \qquad (5)$$

where d_l and d_u are the large- and small-end diameters, d and l are intermediate diameters and lengths at, for example, the critical point and k scales diameter to the same units as length. Log form is controlled by the parameter r, with $0 < r < 2$ a neiloid, $r = 2$ a cone and $r > 2$ a paraboloid. In the following examples, the assumed log form is a paraboloid with $r = 3$. The log length and large-end diameters are also held constant at $L = 8$ m and $d_l = 0.5$ m, while the upper log diameter is allowed to vary $0 < d_u \leq d_l$ as noted in each example.

Large-end protocol

The large-end estimator protocol has been previously described and is illustrated in Figure 3, while the estimator was given in equation (2). Figure 4a shows the sampling surface for the large-end estimator protocol when the small end of the log tapers to $d_u = 0$. In this figure and those to follow, the log is situated such that the large end is at $(x,y) = (0,0)$, and the small end is at $(8,0)$.

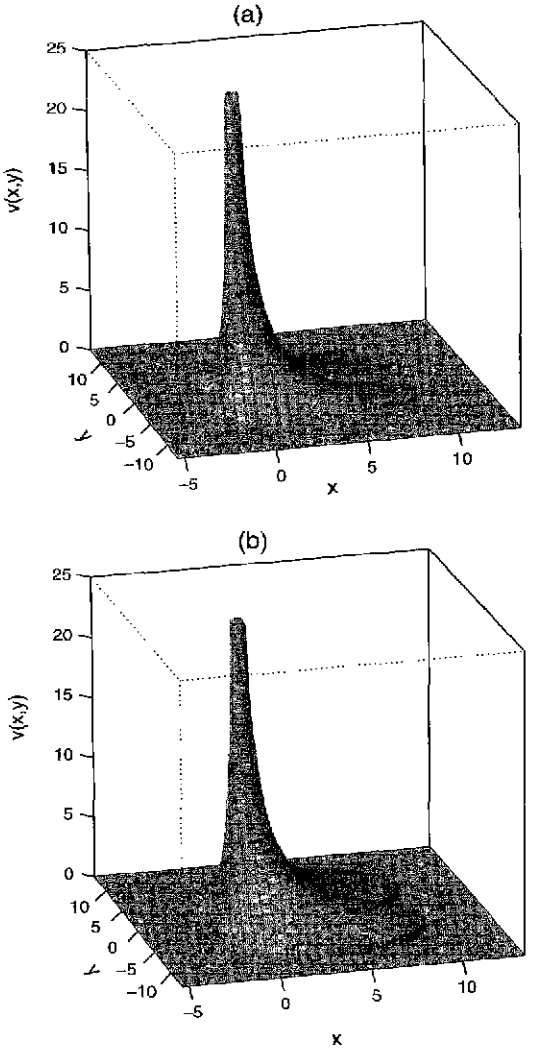

Figure 4. Sampling surfaces (truncated) for large-end protocol using a relascope angle of $\nu = 45°$: the large end of the log is situated at (0, 0); $L = 8$ m and $d_l = 0.5$ m with (a) $d_u = 0$ m and (b) $d_u = 0.3$ m.

The surface has been artificially truncated to $\max(\hat{v}(x, y)) = 25$ for display purposes only, to facilitate comparison among the methods. While this surface has been generated from exhaustive sampling, it is exactly analogous to the expanded tree stem surface shown in Figure 1 for CHS, which was generated analytically as a constant function of tree diameter along the stem. Notice that the surface is extremely uneven and reaches a peak (singularity) at the large end of the log, where the sampling point (grid cell) happens to fall very close to the centre of the large-end diameter of the log; this singularity is a result of the critical length approaching zero. The surface volume quickly recedes towards the small end and outwards, away from the log. One can faintly discern the outline of the PRS inclusion zone for the entire log from the shadows cast by the surface in this figure.

Figure 4b shows another surface, this time with the log tapering to a small-end diameter of $d_u = 0.3$ m. Notice that, while the surface behaviour is still the same at the large end, the surface is noticeably higher at the small end of the log. Inspection of equation (2) shows that this is due to the fact that at any given critical length, the critical diameter is larger for this log than that of the previous example, and therefore so is the estimate of volume produced, all other things being equal. The sampling surface for this truncated log clearly shows the outline of the PRS inclusion zone, which was only faintly visible in the first log.

Small-end protocol

As an alternative to the large-end protocol, it is possible to align one side of the projected relascope angle with the small end of the log, rather than the large end. Under this protocol, the critical point is similarly defined as the point where the other leg of the projected angle intersects the log. The natural question to ask is whether the use of this protocol has any effect on the resulting estimate of volume? It was mentioned above that this protocol is also unbiased, but the variance could be different due to the change in definition of the critical point itself along the log. This idea is explored further in this section.

The small-end protocol is illustrated in Figure 5. Because the critical point determined with this protocol will be different than the critical point determined by the large-end protocol, the CPRS small-end estimator for volume is defined as

$$v'' = cA\mathcal{L}\sum_{i=1}^{n}\frac{d_i''^2}{l_i''}, \quad l_i'' > 0,$$

where d'' and l'' are the critical diameter and length, respectively, using the small-end protocol.

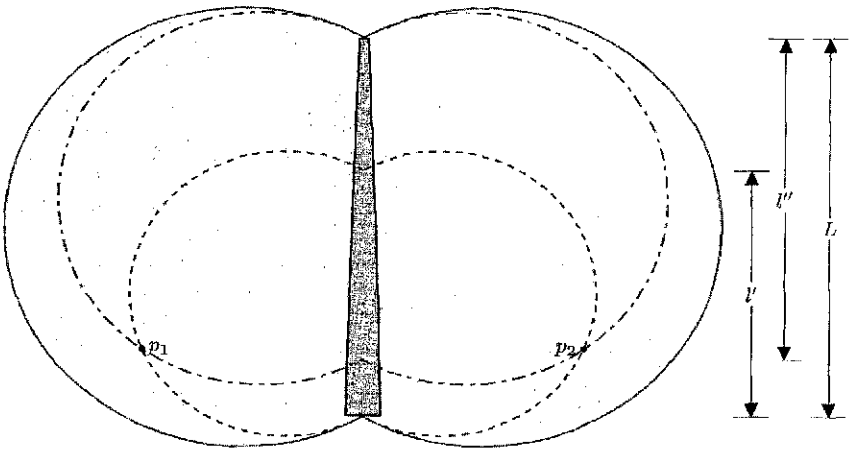

Figure 5. CPRS geometry with an gauge angle of $v = 60°$ for three protocols: large end (dashed) with critical length l', small end (dashed–dotted) with critical length l'' and antithetic points p_1 and p_2 combining the two.

The sampling surfaces generated with this estimator protocol are shown in Figure 6 and are directly comparable with the large-end surfaces in Figure 4. The actual statistics for the corresponding surfaces are shown in Table 1. The surface appears markedly different for the small-end protocol when the top diameter tapers to zero (Figure 6a). When the sampling point falls near the small end of the log, both the critical diameter and the length are small, so the surface goes to zero as the critical point approaches the tip since $d''^2 \to 0$ faster than l''. As the critical point approaches the large end of the log, both diameter and length increase, and the proportional rate of increase in d''^2 over l'' is relatively small, producing a maximum height of the surface that is dramatically less than that for the large end (Table 1). In Figure 6b, $d_u = 0.3$ m, and the sampling surface resembles that of the large-end protocol, but again, much reduced in height because $d_u < d_l$. Intermediate between the two, as the small-end diameter increases, the sampling surface appears to melt around the edges in Figure 6a while slowly building a spike at the small end, until it resembles Figure 6b.

Williams (2001) notes that the evenness of the sampling surface is directly related to the variance; this can be seen by inspection of equation (3). As a result of the large peak in the surface under the large-end protocol, the sampling surface is very uneven as compared to the respective small-end surfaces. Consequently, the large-end protocol has higher variance than the small-end protocol for the log in question as shown in Table 1. Note that even the relative variability, as judged by the coefficient of variation, is always higher for the large-end protocol and is useful for comparing logs of differing dimensions within a common protocol. The simulations will address whether these results hold true for a larger population of logs.

Antithetic protocol

Antithetic sampling was introduced in connection with CHS and importance sampling by Van Deusen and Lynch (1987) as a means of reducing the variance of the proposed estimators. The general reasoning was that when subsampling a log for volume estimation, if more than one measurement is to be taken, it would be better to take one measurement near the small end and one near the large end, rather than taking them both nearby, at say, the middle (Van Deusen, 1990). This follows because sampling at the extremes using antithetic pairs introduces negative correlation into the variance and therefore is a variance reduction technique (Rubinstein, 1981, p. 135). When sampling measurement locations from a uniform probability density with random variable

$U \in [0, L]$, for example, the diameters sampled at $d(u)$ and $d(1-u)$ form an antithetic pair. The two protocols presented above naturally lead to a kind of antithetic sampling when they are combined; that is, one would take pairs of measurements by employing the large- and small-end protocols on a given log. This is illustrated in Figure 5 where the points p_1 and p_2 both select the same antithetic pair of sampling points (d', l') and (d'', l''). Unlike the preceding two protocols, where PRS points can fall anywhere along the periphery of the CPRS zones, p_1 and p_2 are the only two such PRS points that select these antithetic pairs. In addition, rather than sampling from a uniform density, sampling is from equation (1) for each of the two points. The proposed estimator combines the antithetic pair as a simple average, viz.

$$v''' = cAC\sum_{i=1}^{n} \frac{d_i'^2 l_i'' + d_i''^2 l_i'}{2 l_i' l_i''}, \quad l_i', l_i'' > 0.$$

Because both v' and v'' are unbiased, v''' will also be unbiased (Rubinstein, 1981, p. 135).

It is straightforward to envision the sampling surfaces generated with this protocol because they are simply the average of large- and small-end surfaces taken at each respective grid cell. If Figures 4a and 6a are compared, for example, it is clear that the surface from the large-end protocol will dominate that of the small-end protocol (Figure 7a). Likewise, comparing the variance of the antithetic protocol with the other two in Table 1 shows no gain over the small-end estimator for a log that tapers to the tip. However, as the small end of the log becomes more and more truncated, all other things being equal, so that the log becomes more cylindrical, the variance of the antithetic estimator decreases to where it is lower than the small-end estimator. In addition, this result evidently holds for logs of various lengths as is shown in Table 1 for a log where $L = 2$ m and $d_u = 0.4$ m (Figure 7b).

Finally, it is worth noting that the pairs of critical points generated by this form of antithetic sampling may not always be negatively correlated. Referring once again to Figure 5, one can envision PRS points within the log's inclusion zone where the small- and large-end protocols could choose critical points on the log that are close together.

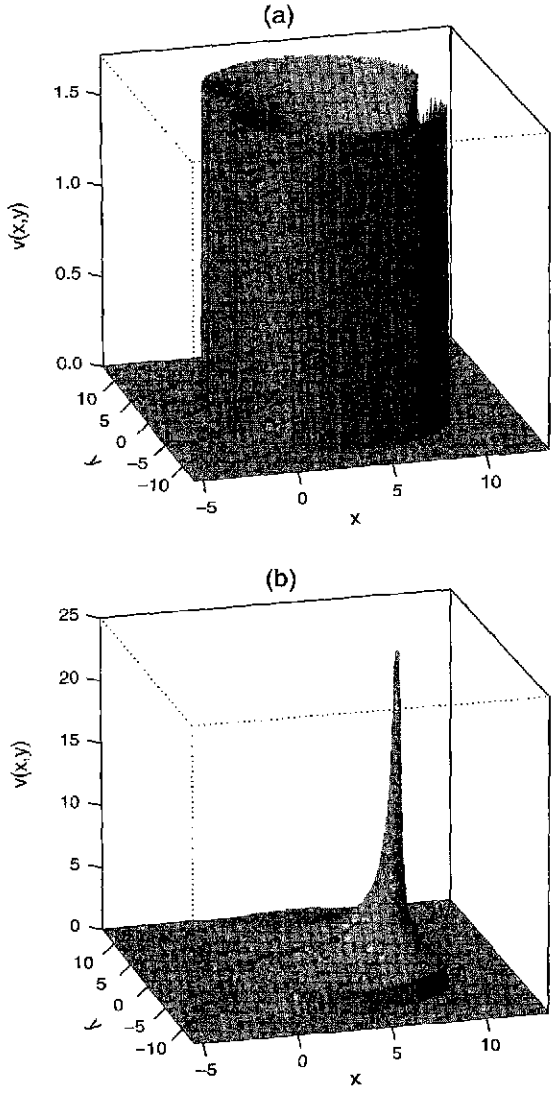

Figure 6. Sampling surfaces for small-end protocol using a relascope angle of v = 45°: the large end of the log is situated at (0, 0); $L = 8$ m and $d_l = 0.5$ m with (a) $d_u = 0$ m and (b) $d_u = 0.3$ m.

In such cases, the antithetic estimate would gain nothing over the small-end protocol variance-wise, regardless of the taper model. In this sense, one might think of the protocol described in this section as a pseudo-antithetic sampling approach,

Table 1: Sampling surface comparison of CPRS estimator protocols for a log with d_1 = 0.5 m and parabolic taper (r = 3); relascope angle υ = 45°

Protocol	d_u (m)	V (m³)	$\bar{V}$ (m³)	sd($\hat{v}(x,y)$)* (m³)	cv(V)† (%)	max($\hat{v}(x,y)$) (m³)
L = 8 m						
Large end	0	0.673	0.665	3.407	512	272.7
	0.3	1.126	1.113	3.592	323	274.1
	0.4	1.334	1.319	3.676	279	274.5
Small end	0	0.673	0.666	0.747	112	1.7
	0.3	1.126	1.113	1.793	161	103.5
	0.4	1.334	1.319	2.657	201	179.0
Antithetic	0	0.673	0.666	1.825	274	137.2
	0.3	1.126	1.113	2.160	194	137.9
	0.4	1.334	1.319	2.450	186	138.1
L = 2 m						
Large end	0.4	0.333	0.329	3.382	1028	273.1
Small end	0.4	0.333	0.329	2.673	811	183.6
Antithetic	0.4	0.333	0.329	2.522	766	140.3

* Surface standard deviation: sd($\hat{v}(x,y)$)= $\sqrt{\text{var}(\hat{v}(x,y))}$.
† Surface coefficient of variation: cv(V) = 100 × sd($\hat{v}(x,y)$)/$\bar{V}$.

which has the potential to realize gains in efficiency with a little extra measurement effort when judiciously applied in the field.

In general, regardless of the protocol used, the other log shapes given by the taper equations (4) will tend to generate sampling surfaces that are similar to the ones illustrated in the overall form. However, because taper can vary quite substantially between the neiloid and a fat paraboloid (e.g. r = 7), there will be some variation in sampling surfaces for logs with similar dimensions under the different taper models when compared for each of the estimators.

Correction for sloped, crooked and forked logs

At this point, the reader may object that much of the presentation above seems to assume straight, unforked logs lying on perfectly level terrain. This assumption, of course, is unlikely to be satisfied in practice, but it is not a necessary assumption for the correct and unbiased implementation of the method. What is required is that the log can be defined relative to a straight, unforked axis, so that the expectations and integrals in the development above are defined relative to the projection of the log onto that axis. In the field, that assumption can be satisfied exactly through a simple, unified correction procedure. The procedure and its rationale follow the work of Williams *et al.* (2005b) closely.

Define the *log needle* as the line segment within a convenient horizontal plane, joining the projection of the two endpoints of the log into that plane; likewise, let $\mathcal{L}$ also be defined on that plane. Projection of all the measurements of the log onto that needle can be accomplished easily in the field, and corrects for sloped, crooked and forked logs.

Correction for sloped logs

Suppose that the log is straight and elevated above (or below) the log needle. If l' and l'' are measured in terms of the log needle, and the cross-sectional area is measured in the plane normal to the needle (i.e. vertically), then the proofs given above still hold. If either d' or d'' are measured with calipers, this does require operating the calipers vertically rather than perpendicular to the axis of the physical log. It will also typically require measuring more than one diameter to establish the cross-sectional area of the log, as a vertical section through a sloping log will tend to be elliptical rather than circular.

Correction for crooked logs

Suppose that the log is deflected away from the log needle by some curve or sweep. If l' and l'' are measured in terms of the log needle, and the cross-sectional area is measured in the plane normal to the needle, then the proofs given above

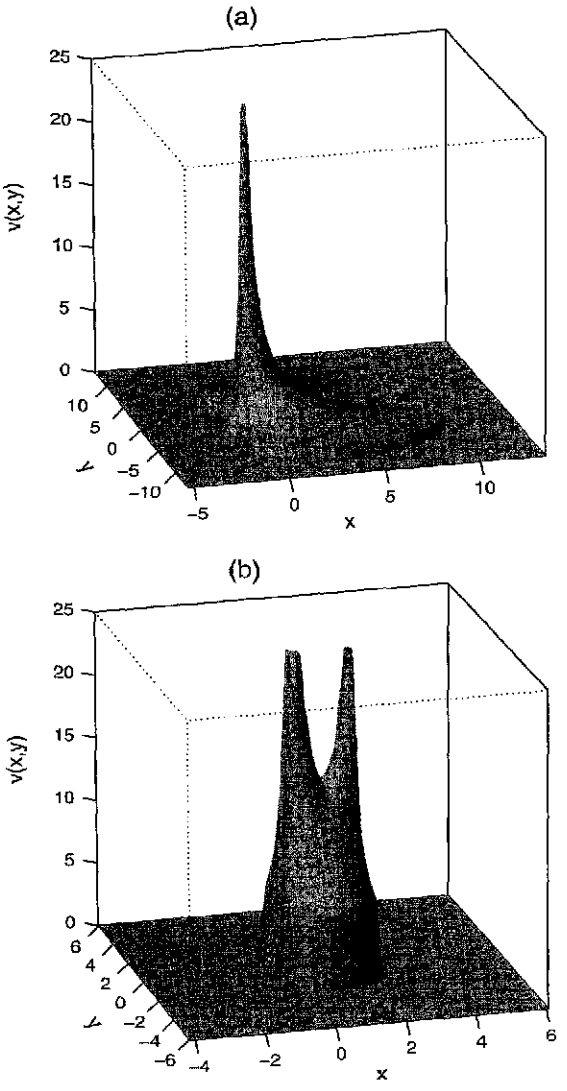

Figure 7. Sampling surfaces for antithetic protocol using a relascope angle of $\nu = 45°$: the large end of the log is situated at (0, 0); $d_l = 0.5$ m with (a) $L = 8$ m and $d_u = 0$ m and (b) $L = 2$ m and $d_u = 0.4$ m.

still hold. This may require additional fieldwork to identify the critical point on the needle, which now may not coincide with the log, and also to project the plane perpendicular to the log needle, onto the log to establish the location for diameter measurement.

Correction for forked logs

Suppose that the log ramifies. Given any suitable *a priori* definition of what constitutes the two 'ends' of the log, a log needle can still be identified. For example, the basal end of the needle might remain the same, but the distal end of the log needle could be defined as the projection of the furthest branch apex from the base onto the horizontal plane. Having defined the needle in this fashion, the log cross-sectional area at the critical point would be taken as the sum of the cross-sectional areas of the branches, measured following the protocols for sloped and crooked logs given above. In other words, the cross-sectional area of the log at the critical point is the sum of the cross-sectional areas of the branches measured in the plane normal to the log needle and passing through the critical point.

These procedures correct for slope, crookedness and forking exactly because the volume of the log equals the integral along the log needle of the log cross-sectional area perpendicular to the needle. These correction procedures merely operationalize the field measurements when the physical log is not exactly coincident with the log needle. Initial selection of a log with any of these conditions under PRS would also require the establishment of the needle as outlined in Gove *et al.* (2002).

Sampling surface simulations

The simulations designed in this section seek to determine whether the observations concerning the estimator protocols based on a single log extend to populations of logs. Specifically, interest revolves around the protocol that will provide the lowest variance for a given population of logs. The simulations also seek confirmation that all estimator protocols are indeed unbiased, as was formally proved for the large-end estimator. The simulation results will hold regardless of the relascope angle used, therefore, and the angle of $\nu = 45°$ was chosen for all simulations.

Each population consisted of a tract A with area $A = 1$ ha, that was divided into grid cells of size 0.15 m, providing an effective sample space of 444 889 grid cells (relascope points). Each of three

Table 2: Sampling surface simulation results of relative bias, $\tilde{B}$, and standard deviation, sd($\hat{v}(x,y)$), for CPRS estimator protocols and PRS, with $v = 45°$ for $N = 50$ logs; relative efficiency ($\tilde{E}$) is given in parentheses where applicable

	Neiloid ($r = 1$)		Cone ($r = 2$)		Paraboloid ($r = 3$)	
Protocol	$\tilde{B}$	sd($\hat{v}(x,y)$) (m^3)	$\tilde{B}$	sd($\hat{v}(x,y)$) (m^3)	$\tilde{B}$	sd($\hat{v}(x,y)$) (m^3)
CPRS						
Large end						
Tip	0.989	254.5 (5.06)	0.992	292.3 (3.61)	0.994	270.7 (2.87)
Truncated	0.994	284.8 (2.25)	0.995	362.8 (2.23)	0.995	303.1 (2.02)
Small end						
Tip	0.993	59.0 (1.17)	0.997	86.2 (1.06)	0.998	95.0 (1.01)
Truncated	0.996	162.7 (1.29)	0.997	204.3 (1.25)	0.997	193.8 (1.29)
Antithetic	0.997	159.7 (1.27)	0.997	196.1 (1.20)	0.997	180.8 (1.21)
PRS						
Tip	0.996	50.3	0.997	80.9	0.998	94.2
Truncated	0.996	126.1	0.998	162.9	0.998	149.7

different taper models based on equations (4) was used for comparison: neiloid ($r = 1$), cone ($r = 2$) and paraboloid ($r = 3$). For each of the three taper models, $N = 50$ logs were generated in two sets of populations with random placement and orientation within the respective population. In the first population, all logs were allowed to taper to the tip. In the second, logs were randomly truncated to some small-end diameter $0 \le d_u \le d_l$. The same two populations were then used for small- and large-end protocols, and for truncated logs only, the antithetic protocol. The large-end diameter of the logs was chosen as Uniform(0, 1) m, while the log length was Uniform(0.15, 6.8) m. In the simulations where the anithetic protocol was used, it was applied only to the subsample of logs that met the condition $d_u \ge 0.7d_l$, based on the findings of the last section.

If the true volume of the log is known, PRS is unbiased for volume estimation. In addition, it should always have a variance smaller than the critical point-based methods proposed here. This is easy to visualize because the sampling surface for a log under PRS resembles the union of two cylinders with height $\mathcal{L}AV/L^2$ (Williams and Gove, 2003); such a surface will always be smoother (lower variance) for a given population of logs than those generated by CPRS protocols. Because the true volume V of each log is known from equation (5) and its true length L is also known, PRS provides a standard for comparison for the proposed CPRS methods. The interested reader may consult Williams and Gove (2003) for simulations showing how PRS performs with regard to efficiency, relative to other commonly used methods when sampling for CWD volume.

The results are presented in Table 2. For each of the methods, the relative bias was computed as

$$\tilde{B} = \frac{\bar{V}}{\sum_{i=1}^{N} V_i},$$

where the appropriate value for $\bar{V}$ is substituted from the simulation results for each method, including PRS. The variability is judged in terms of the simulation standard deviations ($\mathrm{sd}(\hat{v}(x,y)) = \sqrt{\mathrm{var}(\hat{v}(x,y))}$) as in the individual log results of Table 1. In addition, the relative efficiency, defined as

$$\tilde{E} = \frac{\mathrm{sd}(\hat{v}(x,y))}{\mathrm{sd}(\hat{v}(x,y))^*},$$

where the denominator is with regard to PRS, is also given.

It is important to note that the relative bias can only be exactly unity if the surface integral is computed exactly for an unbiased method. Approximating the integral by sampling from a grid is analogous to approximation with a Reimann sum. Therefore, for unbiased methods, the degree to which the statistics $\tilde{B}$ depart from unity is based on the resolution of the sampling surface, but they should be close. With this in mind, it is clear that

all the simulations for each CPRS protocol, and for PRS, confirm the unbiasedness of these methods. On the other hand, the difference in variability between the different protocols is striking. In general, the large-end protocol produces the highest variability, regardless of log truncation. For all methods, the variability is smaller for logs that taper to the tip. This is undoubtedly due to the fact that random truncation of logs introduces larger differences in volume between logs, and thus produces a larger population variance. For logs that taper to the tip, the small-end protocol produces results nearly equal to PRS in terms of efficiency. For truncated logs, variability is 25–30 per cent higher than PRS. The antithetic protocol does indeed reduce the variance when compared with the large-end protocol, but the reduction is marginal when compared with the small-end protocol.

The simulation results are consistent across taper models and, because these models encompass most of the geometrical models often applied to logs in terms of tree sections, it is reasonable to expect that similar results will apply to populations of real downed CWD in the absence of advanced decay. In addition, because of the similarity between the single log and population conclusions, it is reasonable to expect that the results would hold for larger populations as well.

Discussion and conclusions

CPRS has been shown, both analytically and through simulations, to be a design-unbiased method for volume estimation in PRS surveys of downed CWD. However, unbiasedness alone is not necessarily beneficial in an estimator if that estimator has inherently high variance. The PDF of the CPRS estimator produces a naturally uneven surface, yielding high variability, most notably with regard to the large-end protocol. The small-end protocol's variance is markedly less for the same population of logs, but still suffers from high variability when the population is highly variable in the sense of log sizes; adding the second antithetic measurement contributes a further small reduction in variance. When all logs taper to the tip, the small-end protocol performs almost as well as PRS with known volume – i.e. it is unbiased and has similar variance properties. Across log taper models, all CPRS estimators perform worst, in terms of relative efficiency, on the population of neiloid-shaped logs. Fortunately, only a small component of tree form, in the area of butt-swell near the base, conforms to such models.

The antithetic estimator protocol produced marginal gains in efficiency over the simple small-end protocol. However, if it is applied based on a rule such as that used in the simulations, one would only be using it on a portion of the logs in the sample. It is difficult to judge whether it would be worth the extra effort in practice. This certainly depends on the form and distribution of the log attributes in the population in question, and whether taking the extra measurements for a small decrease in variance is in line with the goals of the inventory. If it is important to get unbiased minimum variance (among extant methods) estimates of downed CWD volume, PDS should be used. Alternatively, some form of subsampling using importance sampling could be considered. However, in all methods, the downed material in question is assumed to be relatively free from decay. For logs in advanced stages of decay where deflation, crumbing and the like have altered the solid content and original form, none of the methods can be applied without some degree of modification or augmentation to arrive at true estimates of volume.

Unbiasedness of the critical height method for standing trees has been proved in the past by the use of the shell integral. Attempts at using the shell integral for CPRS failed to show unbiasedness in the simulations, even though it appeared that the method provided unbiased estimates analytically. The reasons for this are unknown, but the shell integral, if revisited, might provide a more homogenous sampling surface, and hence lower variance in practice. In addition, Van Deusen and Lynch (1987) arrived at similar conclusions regarding the high variability of CHS when applied independently with one measurement per tree, through an analysis of sample size comparisons. Using a simpler version of equations (4), they found that antithetic sampling dramatically reduced the sample size required for CHS, and therefore the variance as well. Because our version of antithetic sampling relies on the relascope and a non-uniform sampling PDF, our results do not show the profound reduction in variance associated with the technique. In addition, our limited simulations may

not do justice to the antithetic approach compared with sampling many hundreds of logs on a larger inventory.

Finally, while not being explored here, it was mentioned earlier that the mean of the CPRS PDF occurred at a point $2L/3$. This was developed in terms of the large-end estimator, but applies equally to the small-end protocol. Simple repeated sampling from equation (1) shows that this length is indeed realized on average. Thus, it could also provide a simplified measurement point for volume estimation on every log under PRS. It may be that this is found to be similar to centroid sampling for standing trees (Wood *et al.*, 1990). The drawback to this method would be the necessity to locate the critical point at two-thirds the log length on each log with a good degree of accuracy in order for the method to remain unbiased. This would undoubtedly require the extra measurement of total log length at a minimum. However, if an estimate of other quantities under PRS, such as number of pieces or length per unit area, is desired for the inventory overall, total log length will be a required measurement regardless.

In summary, the small-end protocol with possible augmentation of the antithetic point on logs that have relatively large small-end diameters provides a design-unbiased extension to the PRS method for the estimation of log volume. In areas where entire trees with excurrent shape have been toppled, such as large wind events, the method would provide an unbiased technique with excellent variance properties approaching PRS with known volume, and thus PDS as well (Williams and Gove, 2003). It is probably best applied on larger inventories where there would be a large total sample of logs, or on quick inventories where variance might be less of a concern. In both cases, its use presumes the use of PRS as the main technique for the downed CWD inventory. Where this is not the case, PDS will provide a design-unbiased estimate of log volume with minimum variance among extant estimators in most practical cases.

Acknowledgements

We would like to thank the two referees, Drs Kim Iles and Timothy Gregoire, for their helpful comments. This project was supported by the National Research Initiative of the USDA Cooperative State Research, Education and Extension Service, grant number 2003-35101-13646.

References

Ducey, M.J., Gove, J.H. and Valentine, H.T. 2004 A walkthrough solution to the boundary overlap problem. *For. Sci.* **50**, 427–435.

Furnival, G.M., Valentine, H.T. and Gregoire, T.G. 1986 Estimation of log volume by importance sampling. *For. Sci.* **32**, 1073–1078.

Gove, J.H., Ringvall, A., Ståhl, G. and Ducey, M.J. 1999 Point relascope sampling of downed coarse woody debris. *Can. J. For. Res.* **29**, 1718–1726.

Gove, J.H., Ducey, M.J. and Valentine, H.T. 2002 Multistage point relascope and randomized branch sampling for downed coarse woody debris estimation. *For. Ecol. Manage.* **155**, 153–162.

Grosenbaugh, L.R. 1958 Point-sampling and line-sampling: probability theory, geometric implications, synthesis. *Occasional Paper* No. 160. Southern Forest Experiment Station, USDA Forest Service, 34 p.

Husch, B., Beers, T.W. and Kershaw, J.A. Jr 2003 *Forest Mensuration.* 4th edn. Wiley, Hoboken, NJ, 443 p.

Iles, K. 1979a Some techniques to generalize the use of variable plot and line intersect sampling. In *Forest Resource Inventories Workshop Proceedings, Volume 1.* W.E. Frayer (ed.). Colorado State University, Fort Collins, CO, pp. 270–278.

Iles, K. 1979b *Systems for the selection of truely random samples from tree populations and the extension of variable plot sampling to the third dimension.* Ph.D. thesis, University of British Columbia.

Kitamura, M. 1962 On an estimate of the volume of trees in a stand by the sum of critical heights. *Kai Nichi Rin Ko* 73, 64–67.

Lynch, T.B. 1986 Critical height sampling and volumes by cylindrical shells. *For. Sci.* **32**, 829–834.

McTague, J.P. and Bailey, R.L. 1985 Critical height sampling for stand volume estimation. *For. Sci.* **31**, 899–912.

Mizrahi, A. and Sullivan, M. 1982 *Calculus and Analytic Geometry.* 1st edn. Wadsworth, Belmont, CA, 1038 p.

Rubinstein, R.Y. 1981 *Simulation and the Monte Carlo Method.* 1st edn. Wiley, New York, 278 p.

Ståhl, G. 1998 Transect relascope sampling – a method for the quantification of coarse woody debris. *For. Sci.* **44**, 58–63.

Ståhl, G., Ringvall, A., Gove, J.H. and Ducey, M.J. 2002 Correction for slope in point and transect relascope sampling of downed coarse woody debris. *For. Sci.* **48**, 85–92.

Ståhl, G., Gove, J.H., Williams, M.S. and Ducey, M.J. 2005 Critical length sampling: a method to estimate

the volume of down coarse woody debris. *Eur. J. For. Res.* (in press).

Valentine, H.T., Tritton, L.M. and Furnival, G.M. 1984 Subsampling trees for biomass, volume, or mineral content. *For. Sci.* 30, 673–681.

Valentine, H.T., Gove, J.H. and Gregoire, T.G. 2001 Monte Carlo approaches to sampling forested tracts with lines or points. *Can. J. For. Res.* **31**, 1410–1424.

Van Deusen, P. 1987 Combining taper functions and critical height sampling for unbiased stand volume estimates. *Can. J. For. Res.* **17**, 1416–1420.

Van Deusen, P. 1990 Critical height versus importance sampling for log volume: does critical height prevail? *For. Sci.* **36**, 930–938.

Van Deusen, P. and Merrschaert, W.J. 1986 On critical-height sampling. *Can. J. For. Res.* **16**, 1310–1313.

Van Deusen, P.C. and Lynch, T.B. 1987 Efficient unbiased tree-volume estimation. *For. Sci.* **33**, 583–590.

Williams, M.S. 2001 New approach to areal sampling in ecological surveys. *For. Ecol. Manage.* **154**, 11–22.

Williams, M.S., Ducey, M.J. and Gove, J.H. 2005a Assessing surface area of coarse woody debris with line intersect and perpendicular distance sampling. *Can. J. For. Res.* **35**, 949–960.

Williams, M.S. and Gove, J.H. 2003 Perpendicular distance sampling: an alternative method for sampling downed coarse woody debris. *Can. J. For. Res.* **33**, 1564–1579.

Williams, M.S., Valentine, H.T., Gove, J.H. and Ducey, M.J. 2005b Additional results for perpendicular distance sampling. *Can. J. For. Res.* **35**, 961–966.

Wood, G.B., Wiant, H.V., Loy, R.J. and Miles, J.A.M. 1990 Centroid sampling: a variant of importance sampling for estimating the volume of sample trees in radiata pine. *For. Ecol. Manage.* **36**, 233–243.

Received 22 November 2004